American Mineralogist, Volume 73, pages 727–740, 1988

Fe-Ti oxide–silicate equilibria: Assemblages with fayalitic olivine

B. Ronald Frost
Department of Geology and Geophysics, University of Wyoming, Laramie, Wyoming 82071, U.S.A.
Donald H. Lindsley, David J. Andersen
Department of Earth and Space Sciences, State University of New York, Stony Brook, New York 11794, U.S.A.

Abstract

In Fe-rich metamorphic and highly evolved igneous rocks, quartz can coexist with Fe_2SiO_4-rich olivine. The relationships between these phases and the Fe-Ti oxides are governed by the equilibrium

$$\underset{Quartz}{SiO_2} + 2\underset{Ulvöspinel}{Fe_2TiO_4} = 2\underset{Ilmenite}{FeTiO_3} + \underset{Fayalite}{Fe_2SiO_4},$$

abbreviated QUIIF. For pure fayalite the QUIIF assemblage in equilibrium with metallic Fe is isobarically invariant, falling at 1058 ± 3 °C and $\log f_{O_2} = -14.7 \pm 0.1$ at 1-bar pressure. With increasing f_{O_2}, metallic Fe is lost, and the assemblage becomes isobarically univariant, the ulvöspinel and ilmenite gaining Fe_3O_4 and Fe_2O_3, respectively. The QUIIF assemblage is stable at 942 ± 10 °C and 10^{-14} bars f_{O_2} (WM buffer, 1 bar); at lower temperatures it becomes asymptotic to the FMQ buffer curve. The univariant equilibrium can be expressed by the relation $\ln K_{QUIIF} = 3827/T - 2.868 + 0.0280(P - 1)/T$ (T in kelvins, P in bars; $K_{QUIIF} = [a^2_{Ilm} a_{Fay}]/[a^2_{Usp} a_{Qtz}]$). Above QUIIF, fayalite and ilmenite are not both stable with titanomagnetite and quartz; below QUIIF, quartz and titanomagnetite are not both stable with fayalite and ilmenite. Because QUIIF contains the subassemblage titanomagnetite and ilmenite, it provides redundant information on the temperature and f_{O_2} of formation if the presssure can be estimated to within 1–2 kbar.

If the olivine is not pure Fe_2SiO_4, displacement of QUIIF can be calculated by use of a solution model for olivine. Furthermore, if either fayalitic olivine or quartz is absent from the assemblage, QUIIF can be used to calculate the activity of the corresponding component—provided that pressure is known and that the primary compositions of the oxides can be determined. Likewise, if titanomagnetite or ilmenite is missing, QUIIF provides an estimate of $a_{Fe_3O_4}$ or $a_{Fe_2O_3}$.

The crystallization of a number of volcanic and plutonic rocks appears to have been controlled by the QUIIF equilibrium, with the oxide assemblages broadly reflecting the silica activity. Those fayalite-bearing rocks that contain ilmenite as the sole oxide are invariably silica-saturated; those with ilmenite and titanomagnetite may be either saturated or undersaturated with respect to silica; and most of those with only titanomagnetite are strongly undersaturated and commonly contain nepheline. The QUIIF equilibrium also adds important constraints to geothermometry. It decreases by an order of magnitude the uncertainty in the two-oxide thermometer that results from precision of analysis; it allows one to estimate oxygen fugacity in rocks where the oxides have re-equilibrated; and even in cases for which no textural evidence remains, it can show the extent to which Fe-Ti oxides have re-equilibrated and indicates what the original compositions must have been.

Introduction

The dependence of silicate compositions on oxygen fugacity is hardly a new concept: as early as 1935 Bowen and Schairer noted how increased oxidation would drive Fe into the oxide phase and enrich the silicates in Mg. Osborn (1959) and Carmichael (1967a) also published landmark contributions on the relations between oxide and silicate minerals. However, because of the lack of requisite thermodynamic data, it has been impossible to derive expressions that show how the composition of the silicates and Fe-Ti oxides in a rock co-vary as a function of oxygen fugacity. In our studies of the Laramie Anorthosite Complex we found that whereas two Fe-Ti oxides were apparently stable throughout much of the crystalli-

0003–004X/88/0708–0727$02.00

zation of the complex, Fe-Ti spinel is absent from monzosyenitic rocks with high Fe/Mg ratios. This led us to postulate that the equilibrium controlling the stability of the spinel phase in such rocks is

$$\underset{\text{(quartz or melt)}}{SiO_2} + \underset{\text{(ulvöspinel)}}{2Fe_2TiO_4} = \underset{\text{(ilmenite)}}{2FeTiO_3} + \underset{\text{(fayalite)}}{Fe_2SiO_4}, \quad (1)$$

which we call QUIlF. The importance of this equilibrium was first noted in studies of lunar basalts (see, for example, Taylor et al., 1972; El Goresy and Woermann, 1977), which are sufficiently reduced that the phases approach the end-member compositions. In this paper we use a new calibration of the Fe-Ti oxide geothermometer (Andersen and Lindsley, 1988), together with compatible calibrations of the HM and FMQ buffers (Haas, pers. comm.) and experimental determinations of QUIlF to derive expressions showing the stability of Fe-Ti oxides in the presence of fayalitic olivine. In subsequent papers we will extend the treatment to more magnesian systems and consider the stability relations of assemblages containing pyroxenes and other silicates.

Theoretical considerations

Equilibrium 1 can be expressed by subtracting the QIF buffer

$$\underset{\text{(fayalite)}}{Fe_2SiO_4} = \underset{\text{(iron)}}{2Fe^0} + \underset{\text{(quartz)}}{SiO_2} + O_2 \quad (2)$$

from the reaction for reduction of ulvöspinel:

$$\underset{\text{(ulvöspinel)}}{2Fe_2TiO_4} = \underset{\text{(ilmenite)}}{2FeTiO_3} + \underset{\text{(iron)}}{2Fe^0} + O_2. \quad (3)$$

Graphically, this corresponds to the intersection of curves (2) and (3) in T–log f_{O_2} space to yield the isobarically invariant assemblage Fay + SiO_2 + Usp + Ilm + Fe^0 (point Q in Fig. 1). Early attempts to locate point Q from the intersection of (2) and (3) (e.g., Taylor et al., 1972) were not completely successful because the curves are subparallel and thus small errors in their location yield large uncertainties in the point of intersection. El Goresy and Woermann (1977) located Q directly by reversing (1) in the presence of Fe^0, obtaining $T_Q = 1055 \pm 5$ °C. We have redetermined Q in Fe^0 capsules, obtaining $T_Q = 1060 \pm 5$ °C, in excellent agreement with the value of El Goresy and Woermann (see App. 1 for experimental details). We adopt 1058 ± 3 °C as the optimum temperature for Q; the Haas (pers. comm.) calibration of the QIF buffer yields $\log f_{O_2} = -14.7 \pm 0.1$ for this temperature.

QUIlF, which is the Fe^0-absent univariant curve emanating from Q, is nominally independent of f_{O_2} and would therefore be vertical on a T vs. log f_{O_2} plot (Fig. 1). We could use solution models for ilmenite-hematite and ulvöspinel-magnetite (Andersen and Lindsley, 1988) to calculate the trajectory of (1) away from point Q. A difficulty with this approach lies in evaluating the effects of excess Ti_2O_3 in ilmenite and of excess TiO_2 in ulvöspinel near Q. The data of Simons and Woermann (1978) show that neither ulvöspinel nor ilmenite has its ideal end-member composition at Q: ilmenite contains several percent Ti_2O_3 and ulvöspinel, although lying on the FeO-TiO_2 join, has a slight excess of TiO_2. Furthermore, El Goresy and Woermann (1977) have shown that (3) is strongly curved in the vicinity of the invariant point, a feature that complicates any analytical expression for that reaction. For all these reasons, we have chosen an alternative approach for locating QUIlF.

At oxygen fugacities above Q, QUIlF is displaced as ulvöspinel and ilmenite both gain Fe^{3+} by the substitution $2Fe^{3+}$ for $TiFe^{2+}$. The compositions of the coexisting oxides are governed (Rumble, 1970) by an exchange reaction and the redox equilibrium (MH buffer):

$$\underset{\text{(in ilmenite)}}{6Fe_2O_3} = \underset{\text{(in titanomagnetite)}}{4Fe_3O_4} + O_2. \quad (4)$$

The temperature and f_{O_2} at which a given oxide pair equilibrate can be determined from the magnetite-ilmenite thermometer and oxygen barometer (Andersen and Lindsley, 1988). When quartz and fayalite are also present (QUIlF assemblage), two other equilibria also express the oxygen fugacity:

$$\underset{\text{(in titanomagnetite)}}{2Fe_3O_4} + \underset{\text{(quartz)}}{3SiO_2} = \underset{\text{(fayalite)}}{3Fe_2SiO_4} + O_2 \quad (5)$$

$$\underset{\text{(in ilmenite)}}{2Fe_2O_3} + \underset{\text{(quartz)}}{2SiO_2} = \underset{\text{(fayalite)}}{2Fe_2SiO_4} + O_2. \quad (6)$$

In the pure Fe-Si-O system, (5) is, of course, the familiar FMQ buffer, and (6) is the metastable equilibrium FHQ (fayalite + hematite + quartz), but for the purposes of this paper, the displaced equilibria are more important. The trajectory of QUIlF in T vs. log f_{O_2} space is the locus of points for which Equilibria 4 (two-oxide assemblage), 5 (fayalite + $magnetite_{ss}$ + quartz), and 6 (fayalite + $ilmenite_{ss}$ + quartz) all give the same f_{O_2} at the temperature indicated by the oxides. Activities of Fe_2O_3 in ilmenite and of Fe_3O_4 in titanomagnetite are calculated from the solution models of Andersen and Lindsley (1988). QUIlF must become asymptotic to the FMQ buffer at low temperatures where magnetite is nearly free of Ti when it coexists with ilmenite. Because (6) is a linear combination of (4) and (5), in practice it is sufficient that any pair of the equilibria yield the same f_{O_2} values.

For this approach to be successful, it is imperative that the buffer calibrations be mutually consistent and also be identical to those used in deriving the Fe-Ti oxide solution models. We have therefore adopted MH, FMQ, WM, and FIQ from the compilation by Haas (pers. comm.), the same buffer calibrations used by Andersen and Lindsley (1988) for the Fe-Ti oxide solution models. The expressions used by Haas are quite complex and not readily adaptable for small computer programs. For con-

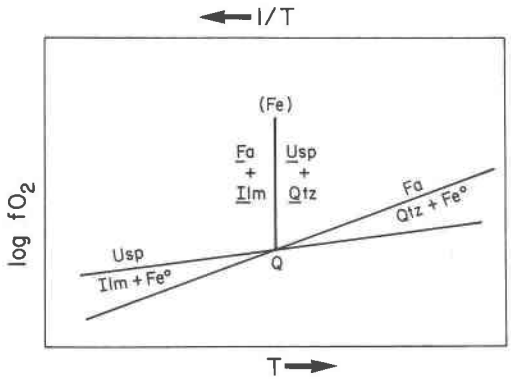

Fig. 1. Topologic relations between the QUIIF reaction and the fayalite-iron-quartz (QIF) and ulvöspinel-ilmenite-Fe° buffers. Point Q represents the coexistence of all five phases.

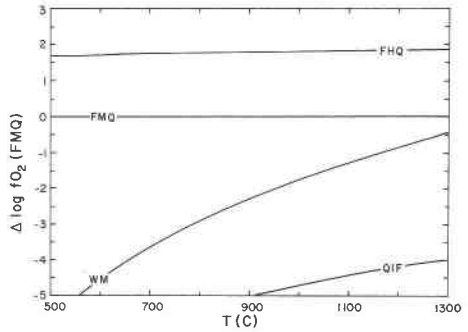

Fig. 2. Location of several common buffers in T–$\Delta \log f_{O_2}$ space. The FHQ equilibrium is metastable and is calculated by combining the HM and FMQ buffers. Calibrations are from the compilation of Haas (pers. comm.).

venience in calculation, we have therefore fitted his values with segments that are linear in $1/T$ vs. $\log f_{O_2}$ space. Table 1 lists the expressions we have adopted for oxygen fugacity. Within its allotted temperature range, each expression deviates from Haas's values by no more than 0.06 log unit. None of these expressions should be used outside its stated temperature range, or serious errors may result.

For several reasons, the f_{O_2} diagrams used in this paper employ the variable $\Delta \log f_{O_2}$ ($= \log f_{O_2} - \log f_{O_2}^{FMQ}$ at the temperature of interest) (Ohmoto and Kerrick, 1977; Frost, 1985). First, many igneous and metamorphic rocks have f_{O_2} values near those of the FMQ buffer (see Haggerty, 1976), so it is a convenient reference. Second, because buffer curves have steep slopes in T vs. $\log f_{O_2}$ space, oxygen fugacity values are virtually meaningless unless they are related to temperature or to one of the buffers. By relating oxygen fugacity to a common buffer, we can show the variation of oxygen fugacity with temperature on a larger scale using the T vs. $\Delta \log f_{O_2}$ projections than can be done on traditional T vs. $\log f_{O_2}$ diagrams. The buffers used in this paper are plotted on such a diagram in Figure 2. A disadvantage in plotting magnetite-ilmenite equilibria on this diagram is that $\Delta \log f_{O_2}$ values have the same pressure correction as FMQ. In calculating $\Delta \log f_{O_2}$ for a system with only small variations in pressure, one may eliminate this pressure dependence by using the pressure of interest as the standard state. In this paper, because we are comparing rocks that formed at a variety of pressures, we have adopted 1 bar as the standard state for $\Delta \log f_{O_2}$.

The actual calculation of the location of QUIIF is simple if inelegant. Because the activity coefficients of the oxide phases are functions of composition, it is not possible to solve directly for f_{O_2} at a given T. Instead, it is convenient to choose pairs of oxides and then to test whether the oxygen fugacities indicated by (4), (5), and (6) agree within a certain tolerance. We use a computer program to cycle through appropriate pairs of compositions ($Ilm_{94-99.9}$ and Usp_{2-99}); when a match is found, the calculated temperature and oxygen fugacity are printed out. The location of QUIIF in the pure Fe-O-SiO_2-TiO_2 system is shown superimposed on the graphical magnetite-ilmenite thermometer in Figure 3a.

The calculation of QUIIF becomes increasingly uncertain at lower oxygen fugacities as the compositions of the titanomagnetite and ilmenite have ever less Fe_3O_4 and Fe_2O_3. The uncertainties reflect both large extrapolations from the reference equilibria [point Q lies approximately 4.7 log units below FMQ (Fig. 3a) and 6.5 below FHQ] and extrapolations of the activity models to compositions outside the region of experimental calibration. Thus, calculation of QUIIF by displacing the FMQ and FHQ equilibria can never give an exact value for Q, because it is impossible to reach the Fe^{3+}-free limit in this manner. Put another way, it is impossible to calculate the Usp_{100} and Ilm_{100} isopleths using the Andersen-Lindsley solution models, yet it is just those isopleths that are necessary to

TABLE 1. Buffers in the system Fe-Si-O

Equilibria

$Fe_2SiO_4 = 2Fe + SiO_2 + O_2$	(QIF)
$2Fe_3O_4 + 3SiO_2 = 3Fe_2SiO_4 + O_2$	(FMQ)
$2Fe_2O_3 + 2SiO_2 = 2Fe_2SiO_4 + O_2$	(FHQ)
$6Fe_2O_3 = 4Fe_3O_4 + O_2$	(MH)

Equilibrium expressions*

Buffer	A	B	C	T range (°C)
αQIF	−29435.7	7.391	0.044	150–573
βQIF	−29520.8	7.492	0.050	573–1200
FMαQ	−26455.3	10.344	0.092	400–573
FMβQ	−25096.3	8.735	0.110	573–1200
FHαQ	−26171.1	11.714	0.067	300–573
FHβQ	−25548.4	10.975	0.080	573–682
FHβQ	−25297.7	10.713	0.080	682–1200
MH	−25497.5	14.330	0.019	300–573
MH	−26452.6	15.455	0.019	573–682
MH	−25700.6	14.558	0.019	682–1100

Note: Temperature of the alpha–beta quartz transition is approximated by the expression $T = 573 + 0.025P$ (T in celsius, P in bars). *Caution:* The buffers may be strongly curved at low temperatures, and it is advised not to extrapolate these expressions below the limits indicated.

* Where $\log f_{O_2} = A/T + B + C(P - 1)/T$ (P in bars, T in kelvins).

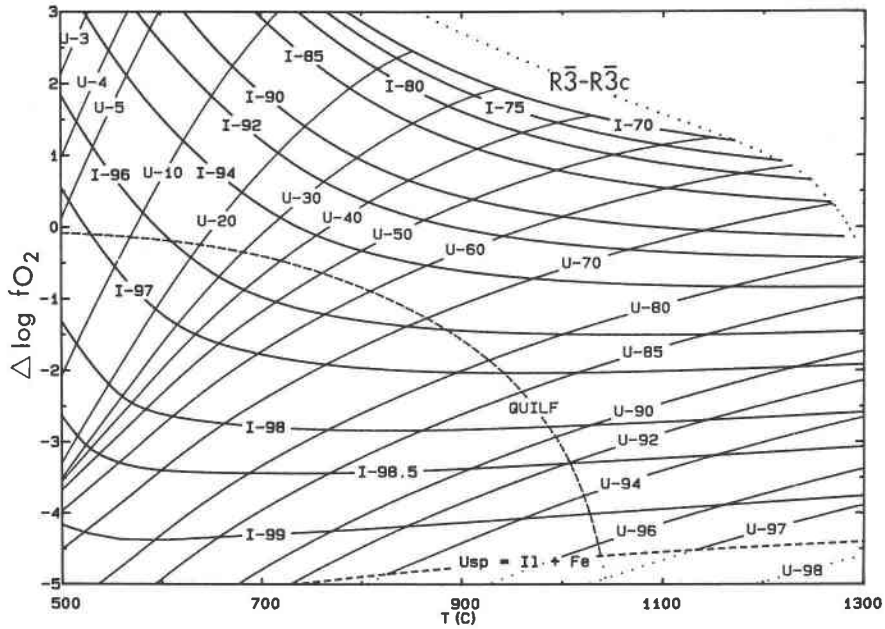

Fig. 3a. T–$\Delta \log f_{O_2}$ diagram showing the location of QUIlF (dashed curve) and the isopleths for X_{Usp} and X_{Ilm} in coexisting Fe-Ti oxides. The dotted line shows the approximate location of the R3̄-R3̄c transition in ilmenites.

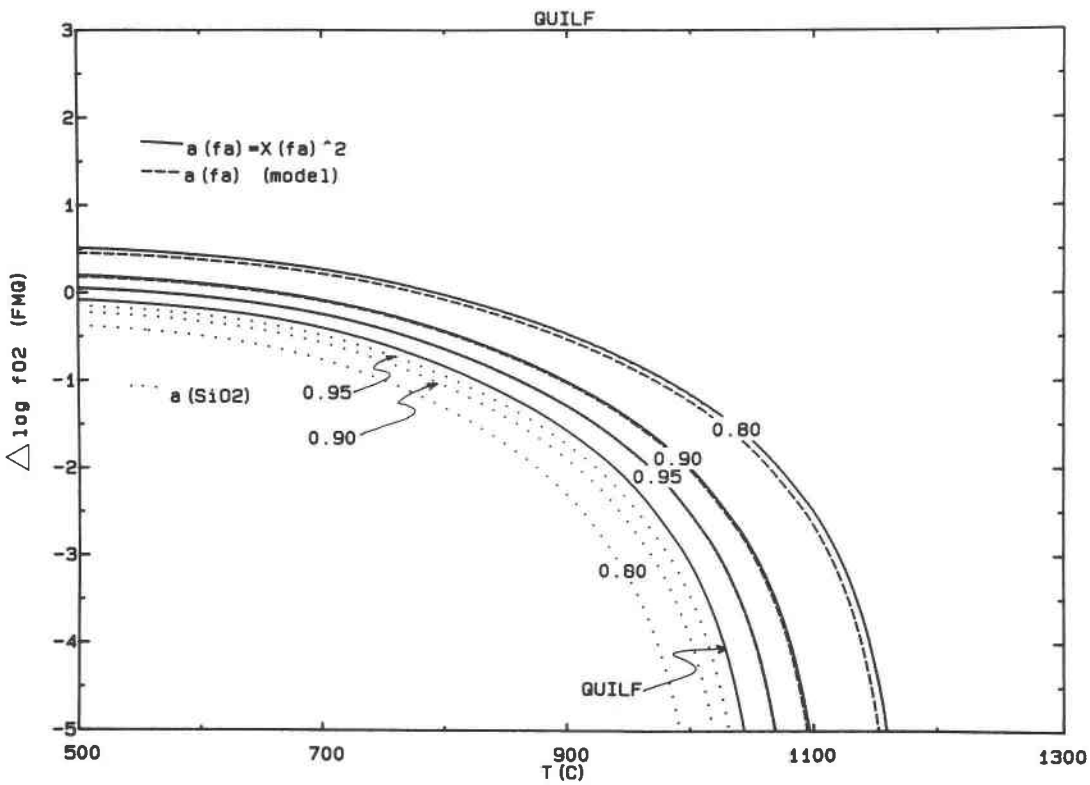

Fig. 3b. T–$\Delta \log f_{O_2}$ diagram showing displacements of QUIlF for various activities of SiO_2 and Fe_2SiO_4. The dashed lines for a_{Fa} use the solution model of Davidson and Mukhopadhyay (1984).

locate Q—even if we ignore the effects of excess Ti present in ilmenite and ulvöspinel at *Q*. The best we can do is to calculate values of QUIIF down to the oxygen fugacity of the QIF buffer; we predict a temperature of 1042 °C for *Q*, compared to the experimentally determined 1058 °C. The agreement is remarkable considering the extent of extrapolation and the fact that the ilmenite and ulvöspinel isopleths intersect at acute angles in this region (Fig. 3a).

QUIIF can be expressed by the equilibrium constant

$$K_{\text{QUIIF}} = [a^2_{\text{Ilm}} a_{\text{Fa}}]/[a^2_{\text{Usp}} a_{\text{Qtz}}]. \quad (7)$$

For the pure system Fe-O-SiO_2-TiO_2 the activities of Fe_2SiO_4 and SiO_2 are unity, and the activities of $FeTiO_3$ and of Fe_2TiO_4 are calculated as outlined above. The natural logarithm of K_{QUIIF} is linear with reciprocal temperature and with pressure, and can be expressed as $3827(9)/T - 2.868(9) + 0.0280(5)(P - 1)/T$ (T in kelvins; P in bars; figures in parentheses show errors in the final digit of each term). If all activities are set to 1, this expression yields $T_Q = 1061$ °C at 1 bar.

The QUIIF equilibrium holds even if quartz or fayalite is absent, or if fayalite is diluted by Mg_2SiO_4 component. Figure 3b shows displacements of QUIIF, with contours for a_{SiO_2} and $a_{Fe_2SiO_4}$. For example, fayalite coexisting with Usp_{30} and Ilm_{96} defines a silica activity (relative to quartz) of 0.8 at 660 °C and $\log f_{O_2} = -18.77$ ($\Delta \log f_{O_2} = -0.70$), the values yielded by the oxides. Likewise, quartz coexisting with Usp_{30} and $Ilm_{94.7}$ defines $a_{Fe_2SiO_4} = 0.8$ at 700 °C and $\log f_{O_2} = -17.06$ ($\Delta \log f_{O_2} = -0.01$). The activity of Fe_2SiO_4 is defined by the solid phases regardless of whether an Fe-rich olivine is present. The exact composition of any coexisting olivine would depend on one's choice of solution model; for Fe-rich olivine at 700 °C the solution would nearly be ideal ($a_{Fe_2SiO_4} = X^2_{Fe_2SiO_4}$), so $X_{Fe_2SiO_4} \cong 0.894$ in the case cited above. As the olivine becomes more forsteritic, two effects are seen. First, and more important, the assemblage olivine + quartz becomes unstable with respect to Ca-poor pyroxene. Second, as the activity of Mg components increases, the oxides themselves become more magnesian (Andersen and Lindsley, 1981). Because Mg is strongly partitioned into olivine compared to the oxides, this effect is relatively unimportant for the Fe-rich rocks considered in this paper.

Application

It has long been recognized that Fe-Ti oxides re-equilibrate on cooling much more readily than do silicates (Buddington and Lindsley, 1964). This re-equilibration can follow any combination of three processes: oxide-silicate reaction, interoxide reaction, and intraoxide reaction. The intraoxide re-equilibration usually manifests itself as "oxy-exsolution" in the titanomagnetite, and its effects can in many cases be compensated for by reintegrating the ilmenite lamellae into the magnetite composition (e.g., Buddington and Lindsley, 1964; Bohlen and Essene, 1977). The detection of an interoxide re-equilibration event is more difficult because this process may leave no petrographic evidence. The occurrence of an interoxide cooling event can be recognized using QUIIF because, in those rocks in which the titanomagnetite has lost Ti on cooling, the reconstructed titanomagnetite composition will not be compatible with the compositions of the coexisting olivine and ilmenite. In such rocks the T and f_{O_2} obtained from oxides alone will be the conditions at which the interoxide re-equilibration ceased.

In the discussion that follows we assume that the oxides form a system closed to oxygen. Under this condition, interoxide equilibration involves the exchange of Fe^{3+} and Ti between magnetite and ilmenite according to the reaction (Rumble, 1970)

$$Fe_2TiO_4 + Fe_2O_3 = FeTiO_3 + Fe_3O_4. \quad (8)$$

The extent to which the compositions of magnetite and ilmenite change by Reaction 8 during re-equilibration, and hence the T and f_{O_2} trend followed, is dependent on the relative proportions of the oxides present. If magnetite is far more abundant than ilmenite, the interoxide cooling trend will follow close to the magnetite isopleths, with ilmenite changing its composition to accommodate Reaction 8. On the other hand, if ilmenite is the dominant oxide, its composition will be largely unaltered during cooling, while the composition of magnetite changes as dictated by Reaction 8. These changes can be quantified by using the reaction progress variable, ξ. By setting X_i to the mole fraction of i in the oxides after a certain amount of reaction has occurred, X^0_i to the initial mole fraction of i in the oxides, and n^0_i to the number of moles of a given solid solution in the initial assemblage, we obtain the following relations:

$$X_{\text{Ilm}} = X^0_{\text{Ilm}} + \xi/n^0_{\text{Ilm}}$$
$$X_{\text{Usp}} = X^0_{\text{Usp}} - \xi/n^0_{\text{Mag}}$$

Normalizing to the abundance of ilmenite and taking into account the difference in the molar volumes (we assume that the volume of the ilmenite solid solution is that of pure ilmenite and that of the magnetite solid solution is the mean of the volumes of pure magnetite and ulvöspinel), we obtain

$$X_{\text{Ilm}} = X^0_{\text{Ilm}} + \xi \quad (9)$$
$$X_{\text{Usp}} = X^0_{\text{Usp}} - \xi/(0.7N), \quad (10)$$

where N = volume of magnetite in the rock divided by the volume of ilmenite. Figure 4, calculated using Equations 9 and 10, shows that both oxides will change composition on cooling unless one phase constitutes only a minute amount of the oxides present, in which case the cooling trend will essentially follow the isopleth for the dominant phase. In the process, ilmenite will become enriched in Ti while magnetite becomes enriched in Fe^{3+}. If the system is not closed with respect to oxygen (that is, f_{O_2} is externally imposed rather than defined by the oxides), the oxide compositions will reflect that f_{O_2}, and thus the actual trends will differ from those in Figure 4.

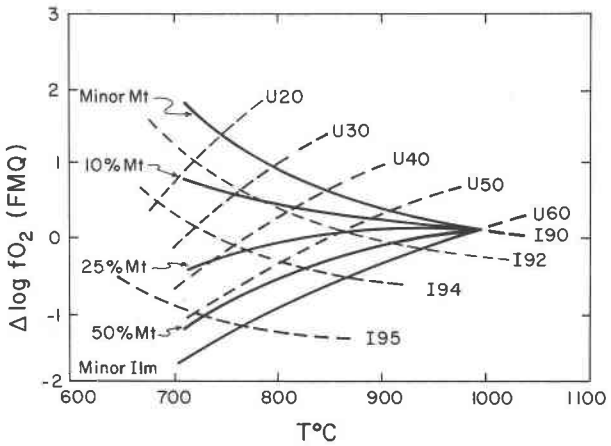

Fig. 4. Cooling trends followed during oxide-oxide equilibration of the same initial oxide *assemblage* but with different proportions of titanomagnetite and ilmenite, assuming that the oxides control the f_{O_2} of the rock (closed system).

There are several ways in which the QUIlF equilibrium can be applied to igneous rocks. Table 2 summarizes the methods that we use, the data that are required, and the information that can be obtained from each technique.

Technique 1. Petrologically, rocks containing two oxides as well as fayalite and quartz are important because the variables T and $\log f_{O_2}$ are overdetermined. Thus, the equilibration conditions of these rocks can be estimated with much more precision than may be possible for rocks with lower variance. Because the system is overdetermined, there are at least two ways one can calculate T and f_{O_2} from a given assemblage. Consider a rock with the assemblage quartz + fayalite ($X_{Fa} = 0.90$) + ilmenite ($X_{Ilm} = 0.950$) + titanomagnetite ($X_{Usp} = 0.75$) that crystallized at 5 kbar. Microprobe analyses are generally accurate to ±1 %. This error converts to an uncertainty of ±1 mol% in the oxides and ±0.2 mol% in olivine. To accommodate this we show isopleths for $X_{Usp} \pm 0.01$ and $X_{Ilm} \pm 0.01$. The small error in olivine composition is ignored because of its negligible effect on the position of the QUIlF surface. Figure 5a gives the location of the isopleths that bound the stability field for this assemblage and shows how QUIlF can be used to refine the T and f_{O_2} estimates obtained from coexisting Fe-Ti oxides. If one uses only the Fe-Ti oxide geothermometer and takes the compositional uncertainties into account, the equilibrium conditions can be estimated to no better than ±88 °C and ±0.3 log unit of f_{O_2}. However, if the constraints of the QUIlF assemblage are added, as defined by the intersections of QUIlF with the spinel isopleths (points *A* and *B*, Fig. 5a), the errors in both estimates are reduced by nearly an order of magnitude. This calculation method, called technique 1 (Table 2), is valid if the composition of the magnetite (either that obtained from homogeneous grains or that obtained by reintegration of oxy-exsolved ilmenomagnetite) can be shown to be compatible with the compositions given for coexisting olivine and ilmenite.

Figure 5b shows the pressure effect on QUIlF and demonstrates that accurate knowledge of pressure is necessary before one can obtain high precision from this technique. Increased pressure has a negligible effect on the T and f_{O_2} conditions estimated from two-oxide geothermometry. Because of the pressure effect on the FMQ buffer, however, increased pressure will affect where these f_{O_2} conditions plot on a T vs. $\Delta \log f_{O_2}$ diagram. The nature of this effect depends on the standard state used: with increasing pressure, $\Delta \log f_{O_2}$ decreases slightly if the standard state is the ambient pressure (dashed lines in Fig. 5b), but increases for a standard state of 1 bar (solid lines). In addition, increasing pressure also displaces the QUIlF surface to progressively higher temperature as one or both oxide phases changes composition. This is illustrated in Figure 5b, which is calculated for $X_{Usp} = 0.75 \pm 0.01$. As a result, if pressure is utterly unknown, the error in the T estimate from the assemblage ilmenite + magnetite + olivine + quartz by technique 1 (Fig. 5b) will be essen-

TABLE 2. Applications of QUIlF

Technique	Data* required	Information obtained
1. Intersection of QUIlF with ulvöspinel isopleths	The assemblage qtz + **ol** + **ilm** + **mt** with concordant temperatures for QUIlF and the Fe-Ti oxide geothermometer	T and f_{O_2} of the oxide-silicate equilibration
2. Intersection of QUIlF with ilmenite isopleths	The assemblage qtz + **ol** + **ilm** + mt with discordant temperatures between QUIlF and Fe-Ti oxide geothermometer	Estimate of maximum T and minimum f_{O_2} of equilibration (if ilm is far more abundant than mt, these values will be very close to actual T and f_{O_2} of equilibration)
3. Intersection of independent geothermometer with QUIlF	Independent geothermometer and either (1) qtz + **ol** + ilm + mt without any oxide composition or (2) **ol** + ilm + **mt** with estimate of primary magnetite	For (1): f_{O_2} For (2): f_{O_2} and a_{SiO_2}
4. Displaced FMQ or FHQ	The assemblage (1) qtz + **ol** + **mt** or (2) qtz + **ol** + **ilm**	Range of f_{O_2} and (1) minimum or (2) maximum T

* Compositions are required for boldface phases.

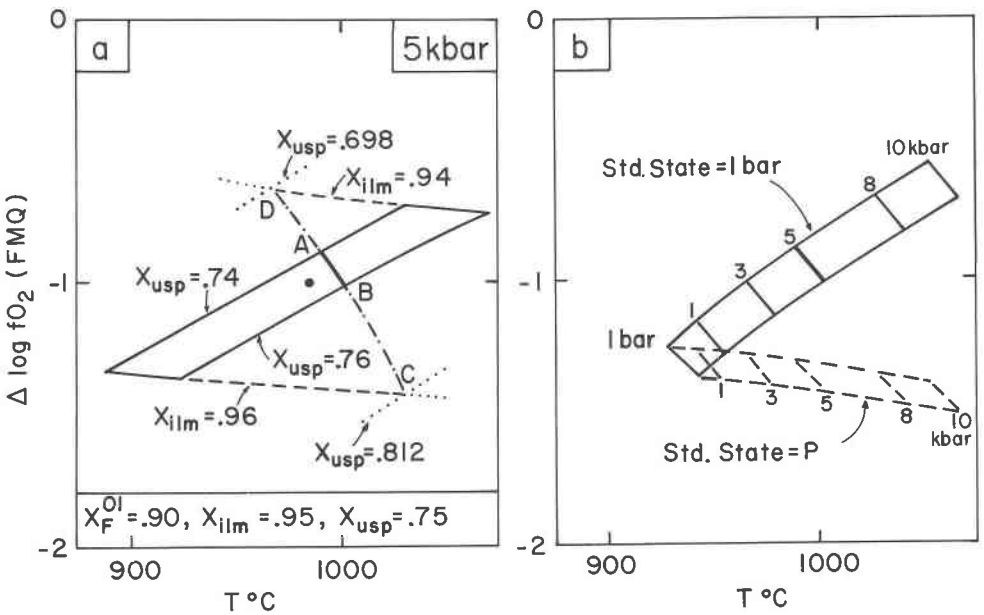

Fig. 5. **(a)** Conditions of equilibrium for a hypothetical rock containing ilmenite, titanomagnetite, fayalite, and quartz at 5 kbar. The solid lines outline equilibrium conditions as estimated from the oxides alone, assuming analytical accuracy of ±1%. Chord *A–B* shows the equilibrium conditions when the constraints of the QUIIF equilibrium are added (technique 1). Chord *C–D* gives the estimates if only the ilmenite and olivine compositions are considered (technique 2). **(b)** The effect of pressure on the T and f_{O_2} estimated using the QUIIF equilibrium for the phases in Fig. 5a. Chord *A–B* from (a)—the trace of QUIIF for X_{Usp} = 0.74–0.76—is plotted for several pressures and two standard states. The pressure effect for two oxides alone is negligible; the displacement of chord *A–B* reflects both the pressure effect on the FMQ reference and slight variations in the composition of ilmenite necessary to maintain the QUIIF equilibrium.

tially the same as that for the Fe-Ti oxide geothermometry alone. Unfortunately, because of the small ΔV for the QUIIF equilibrium and the relatively large uncertainty in the Fe-Ti oxide geothermometry, this assemblage makes only a poor geobarometer (see Nicholls et al., 1971; Ewart et al., 1975). In the example shown in Figure 5b, the estimated pressure of formation for this rock would be 5 kbar ± 5 kbar.

If the interoxide re-equilibration was incomplete, then its occurrence can be documented through careful Fe-Ti oxide geothermometry, which will show the oxide pairs clustered along a linear $\log f_{O_2}$ vs. $1/T$ array (T in kelvins; Morse, 1980). The intersection of such a cooling trend with the QUIIF surface, as displaced to account for pressure and the olivine composition, will provide the temperature and oxygen fugacity at which the silicates and oxides in the assemblage last equilibrated. In rocks where interoxide re-equilibration has been so effective that the interoxide cooling trend cannot be directly detected, the interoxide re-equilibration trend may be estimated by determining the relative abundances of magnetite and ilmenite. Equations 9 and 10 can then be solved for X_i^0 for various values of ξ to give the interoxide cooling trend.

Technique 2. Unfortunately, estimates of the relative abundances of magnetite and ilmenite are not given in most references, so in our compilation we have been unable to calculate the interoxide cooling trends. As a result, for those rocks in which the magnetite composition is incompatible with the reported compositions of olivine and ilmenite, we have estimated their oxide-silicate equilibration conditions from the intersection of the QUIIF surface with the ilmenite isopleths (points *C* and *D*, Fig. 5a). Although this method (technique 2; Table 2) has major inherent errors because of the possibility that ilmenite as well as magnetite has changed its composition on cooling, we think that it still provides valuable information. First, considering the relatively Ti-rich ilmenites in question, the uncertainty range of ±0.01 mol% allowed in the ilmenite composition can accommodate considerable interoxide re-equilibration. Even in rocks where magnetite is the dominant oxide, technique 2 will provide accurate estimates of the oxide-silicate equilibration conditions if the interoxide re-equilibration covered a range of 50 °C or less. In rocks with dominant ilmenite, such as many fayalite-bearing rocks, this permissible range is much larger. Technique 2 is most useful for plutonic rocks, because the conditions estimated by this method provide the maximum T and minimum f_{O_2} at which the oxide-silicate equilibrium locked in.

Technique 3. A third important application of QUIIF comes in rocks where an independent estimate of crystallization temperature is available. In such rocks, the QUIIF equilibrium, as displaced for the olivine composition and estimated pressure, can be used to estimate the

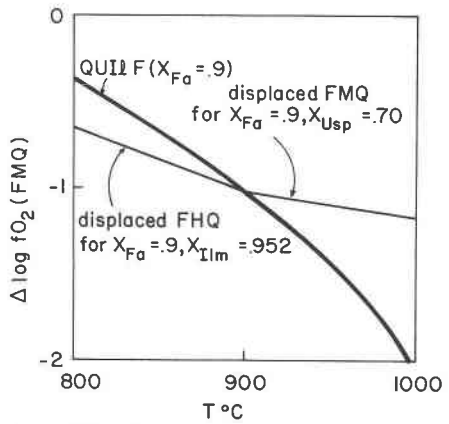

Fig. 6. Use of QUIIF to place maximum temperatures for assemblages without titanomagnetite and minimum temperatures for those that lack ilmenite.

f_{O_2} at which the rock equilibrated (technique 3). This approach is not equivalent to the simple displacement of FMQ, employed by many workers in the past. Displacements of FMQ require knowledge of the primary titanomagnetite composition, which can be reconstructed with certainty only in rocks where no discrete or granular ilmenite is present. However, if ilmenite *is* present, it may be difficult to distinguish primary ilmenite from ilmenite expelled as grains during oxy-exsolution from titanomagnetite and therefore difficult to reconstruct the composition of the primary titanomagnetite. Calculation of f_{O_2} by the intersection of displaced QUIIF with a known temperature, on the other hand, bypasses this problem because it is independent of the present (re-equilibrated) compositions of the oxides. In fact, technique 3 will provide estimates of the original oxide compositions, and thus it enables one to determine whether interoxide re-equilibration has occurred.

Technique 4. A fourth application of QUIIF is to assemblages that contain fayalitic olivine and quartz with titanomagnetite or ilmenite but not both (technique 4). These assemblages must have lain on the FMQ or FHQ curves, as displaced for the compositions of the olivine and of the appropriate oxide. If an independent estimate of either T or f_{O_2} is available, the other variable can of course be estimated. Even without such independent estimates, however, the intersection of displaced FMQ or FHQ with QUIIF (displaced for the composition of the olivine) provides a *minimum* temperature for the titanomagnetite-bearing assemblage or a *maximum* temperature for the ilmenite-bearing assemblage. For example, Usp_{70} and $Ilm_{95.2}$ coexist with Fay_{90} and quartz at 903 °C and $\Delta \log f_{O_2} = -1.05$. If ilmenite is absent, the remaining three phases must have equilibrated above that temperature but along the displaced FMQ curve (Fig. 6). Similarly, if titanomagnetite is absent, the remaining phases must have been in equilibrium below 903 °C and along the displaced FHQ curve.

Discussion

Fayalite-bearing igneous assemblages are most commonly found in highly evolved magmas associated with anorthositic, gabbroic, and alkalic intrusions and in anorogenic granites and rhyolites. The compilations given in Tables 3 and 4 indicate that in igneous rocks, fayalite may occur in the following assemblages:

(1) fayalite + quartz + magnetite,
(2) fayalite + quartz + ilmenite,
(3) fayalite + quartz + ilmenite + magnetite,
(4) fayalite + ilmenite + magnetite,
(5) fayalite + magnetite, and
(6) fayalite + nepheline + magnetite.

It is evident from the stoichiometry of Reaction 1 that the stability of Fe-Ti oxides in the presence of fayalite is a function of both silica activity and oxygen fugacity, as reflected in the assemblages listed above. Apart from one sample from the Skaergaard intrusion (EG-4471), all igneous rocks that are reported in the literature to contain fayalite and quartz also contain ilmenite, suggesting that these rocks crystallized at or below the QUIIF surface. [Although the assemblage fayalite + magnetite + quartz is relatively rare in igneous rocks, it is common in metamorphic rocks, especially high-grade metamorphosed iron formations (see compilation in Frost, 1982). The absence of ilmenite in such rocks reflects their typical very low Ti content; they commonly contain a spinel phase that is nearly pure Fe_3O_4 (Floran and Papike, 1978).]

In rocks with increasingly lower a_{SiO_2}, Reaction 1 will be progressively displaced to the left, stabilizing magnetite relative to ilmenite. From the assemblages listed in Table 4, it is apparent that ilmenite disappears from fayalite-bearing rocks at silica activities somewhat above those limiting the stability of nepheline. In Fe-rich nepheline syenites, therefore, ilmenite is completely lacking, despite the fact that these rocks may form at oxygen fugacities below those of the MW buffer (Powell, 1978) and may contain magnetite with greater than Usp_{80}.

The effects of changing silica activity are well displayed by the Sybille Monzosyenite in the Laramie Anorthosite Complex (Fuhrman et al., 1988). Relatively magnesian portions of this pluton have the assemblage olivine (X_{Fa} = 0.73 to 0.88) + pigeonite + augite plus two Fe-Ti oxides. With increasing Fe enrichment to X_{Fa} = 0.88 to 0.92, pigeonite and magnetite both disappeared while quartz became stable, showing that the conditions of crystallization crossed the QUIIF surface at about the same stage that pigeonite became unstable with respect to augite + fayalite + quartz for the inferred pressure of 3 kbar. The disappearance of titanomagnetite shows that the oxides did not control oxygen fugacity, for otherwise the cooling trend would have been along the QUIIF surface. The oxide + fayalite + quartz assemblages rather were recording f_{O_2} that was controlled by equilibria involving graphite (Fuhrman et al., 1988).

Another example of the effects of silica activity is shown

TABLE 3. Fayalite-bearing mineral assemblages from igneous rocks

Locality	Rock type and association	Assemblage	Ref.†
	Volcanic rocks		
Boina	Pantellerite	ol (Fa_{93}) + ilm ($Ilm_{95.2}$) + mt ($Usp_{50.9}$)	1
Central Victoria	Trachyte	ol (Fa_{70-85}) + Mt ($Usp_{50.7}$)	2
Glen Shurig	Pitchstone dike	ol + ilm + mt + qtz*	3
Kane Springs Wash	Tuff	ol + ilm + mt + qtz*	4
McDermitt caldera	Rhyolite	ol + ilm + mt + qtz*	5
		ol + ilm + qtz*	
Mono Craters	Rhyolite	ol + ilm + mt + qtz*	3
Oraefajokull	Obsidian	ol (Fa_{85}) + ilm ($Ilm_{95.1}$) + mt ($Usp_{63.2}$)	3
Pantelleria	Pantellerite	ol (Fa_{85}) + ilm (Ilm_{95})	3, 6, 7
		ol** + mt (Usp_{61})	
		ol (Fa_{70-85}) + ilm (Ilm_{95-97}) + mt (Usp_{72-77})	
Rondolfur	Pitchstone	ol (Fa_{85}) + mt (Usp_{56})	3
Sierra la Primavera	Rhyolite flows and tuffs	ol + ilm + mt + qtz*	8
		ol + ilm + qtz*	
Eastern Australia	Trachyte	ol (Fa_{97}) + mt (Usp_{41-63})	9, 10
		ol (Fa_{94}) + ilm (Ilm_{98}) + mt (Usp_{56})	
	Rhyolite	ol + ilm + mt + qtz*	
		ol + ilm + qtz*	
Taupo	Rhyolite	ol + ilm + mt + qtz*	10, 11
Thingmuli	Rhyolite	ol + ilm + mt + qtz*	12
	Plutonic rocks		
Bjerkem-Sogndal	Mangerite associated with leuconorite	ol + ilm + mt + qtz**	13
Bushveld	Fe-rich differentiate from layered mafic intrusion	ol + ilm + mt**	14
Fongen-Hullingen	Syenite associated with a layered mafic complex	ol + ilm + qtz**	15
		ol + ilm + mt**	
Kiglapait	Syenite associated with a layered mafic complex	ol + ilm + mt**	16
Klokken	Syenite associated with a gabbroic pluton	ol + ilm + mt + qtz*	17
Skaergaard	Granophyre associated with a layered mafic intrusion	ol + mt + qtz*	18, 19
		ol + ilm + mt + qtz*	
Sybille	Monzonite associated with an anorthosite complex	ol (Fa_{86-92}) + ilm (Ilm_{95-97}) + mt**	20
		ol + ilm + qtz*	
Wolf River	Monzonite associated with anorthosite and anorogenic granite	ol + ilm + qtz*	21
		ol + ilm + mt + qtz*	
Albany, Australia	Anorogenic granite	ol + ilm + mt + qtz*	22
Albany	Quartz syenite associated with anorogenic granite	ol + ilm + mt + qtz*	23
Conway	Anorogenic granite	ol + ilm + mt + qtz*	23
Pikes Peak	Anorogenic granite	ol + ilm + mt + qtz*	24
South Greenland	Fe-rich bodies associated with anorogenic granite	ol + ilm + mt + qtz*	25
Tugtutoq Younger Giant Dyke	Ferrosyenite differentiated from olivine gabbro	ol ($Fa_{<98}$) + ilm + mt + qtz	26
Tugtutoq Older Giant Dyke	Nepheline syenite	ol (Fa_{83-94}) + mt (Usp_{11-16})	27
Coldwell	Syenite associated with an alkalic complex	ol (Fa_{71-91}) + mt (Usp_{44-83}) + ne	28
Igdlerfigassalik	Nepheline syenite	ol (Fa_{93-95}) + mt (Usp_{65}) + ne	29
Ilimaussauq	Nepheline syenite	ol (Fa_{89-93}) + mt (Usp_{13-28}) + ne	30

* See Table 4 for detailed chemistry.

** Analyses not given.

† References: (1) Bizouard et al., 1980; (2) Ferguson, 1978; (3) Carmichael, 1967a; (4) Novak and Mahood, 1986; (5) Conrad, 1984; (6) Wolff and Wright, 1981; (7) Mahood, pers. comm.; (8) Mahood, 1981; (9) Ewart, 1981; (10) Ewart, personal communication; (11) Ewart et al., 1975; (12) Carmichael, 1967b; (13) Duchesne, 1972; (14) Atkins, 1969; (15) Thy, 1982; (16) Morse, 1980; (17) Parsons, 1981; (18) Naslund, 1984; (19) Vincent and Phillips, 1954; (20) Fuhrman et al., 1988; (21) Anderson, 1980; (22) Stephenson and Hensel, 1978; (23) Whitney and Stormer, 1976; (24) Barker et al., 1975; (25) Frisch and Bridgwater, 1976; (26) Upton and Thomas, 1980; (27) Upton et al., 1985; (28) Mitchell and Platt, 1978; (29) Powell, 1978; (30) Larsen, 1976.

by the Tugtutoq Older Giant Dyke (Upton et al., 1985), in which ilmenite disappeared during differentiation. The (earlier) border group of this dike contains olivine (Fo_{53-16}) plus augite and two Fe-Ti oxides, whereas the later central group contains fayalitic olivine (Fo_{10-4}) + augite + nepheline + magnetite without ilmenite. Here it is evident that differentiation of this magma led to a strong increase in Fe activity, with a concomitant decrease in silica activity, displacing Equilibrium 1 to the right and destabilizing ilmenite. For the central group rocks, we can place only an upper limit on f_{O_2}—the appropriate magnetite isopleth in Figure 3a.

The equilibration conditions of fayalite + quartz–bearing rocks reported in the literature are shown in Figures 7–9. The figures were constructed using the procedures discussed above. Where possible, technique 1 or 3 was used, but for those rocks in which the composition of the titanomagnetite is incompatible with the corresponding ilmenite and olivine or in which there is only a limited compositional range over which the minerals are compatible, we used technique 2. Pressure estimates from the original papers were used whenever available; otherwise we assumed the pressure to have been between 500 and 5000 bars. Table 3 lists the pressures used in the calculations; the compatible compositions obtained for each sample are plotted on Figures 7–9.

Several conclusions can be derived from Figures 7–9. Magnetite-bearing rocks equilibrated at higher f_{O_2} than

TABLE 4. Fayalite-bearing mineral assemblages from quartz-saturated igneous rocks

A. Volcanic rocks with the assemblage fa + ilm + mt + qtz

Locality	Sample no.	Observed X_{Fa}	Observed X_{Usp}	Observed X_{ilm}	Calculated X_{ilm}*	Calculated X_{Usp}**	Remarks	Ref.†
Mono Craters	CAM 99	0.895	0.409	0.943	0.9332–0.9424		$P < 3.5$ kbar from QUILF	3
	CAM 73	0.893	0.433	0.945	0.9356–0.9416		$P < 2.5$ kbar from QUILF	3
Taupo	A10	0.848	0.593	0.944	0.9340–0.9392		$P < 2.0$ kbar from QUILF	10
Sierra la Primavera	193	0.94 (est.)	0.483	0.938	0.9326–0.9452			7
Glen Shurig	AC 7	0.853	0.565	0.939	0.9288–0.9386		$P < 3.5$ kbar from QUILF	3
McDermitt caldera	CC-78-130	0.887–0.930	0.594–0.696	0.927–0.979	0.930–0.9524			5, 31
Eastern Australia	87	0.9076	0.634	0.947	0.9384–0.9468		$P < 3.5$ kbar from QUILF	9, 10
	L1670	0.893	0.846	0.984		0.873–0.976		9, 10
Kane Springs Wash	V1-B12	0.948	0.612	0.948	0.9382–0.9486		$P < 4.5$ kbar from QUILF	4
Thingmuli	G151	0.882	0.615	0.946	0.9366–0.9380		$P < 3.0$ kbar from QUILF	12

B. Plutonic rocks with the assemblage fa + ilm + mt + qtz

Locality	Sample no.	Observed X_{Fa}	Observed X_{Usp}	Observed X_{ilm}	Calculated X_{ilm}*	Calculated X_{Usp}**	Remarks	Ref.†
Conway	unnumbered	0.943	0.205–0.247	0.891–0.941	0.9388–0.9472		$P = 1$–2 kbar	23
Albany	unnumbered	0.943	0.293	0.938–0.974	0.9432–0.9480		$P = 1$–2 kbar	23
Klokken	laminated syenite	0.90–0.94	0.5	0.95	0.9402–0.9432		$P = 1$ kbar	17
Pikes Peak	B65D	0.930	0.059	0.938		0.221–0.690	$P = 1$–2 kbar	24
	B65DS	0.934	0.017	0.942		0.170–0.727		24
	B65F	0.941	0.010	0.949		0.220–0.780		24
South Greenland	49,297	0.902	0.014	0.967		0.7936–0.902	$P = 4$–5 kbar	25
	49,082	0.895	0.044	0.970		0.8124–0.916		25
Wolf River	GR-17B	0.950	0.080	0.985		0.880–0.9782	$P = 3$–4 kbar from fa + pig + aug + qtz	32
Albany Australia	unnumbered	0.924	0.427	0.97		0.804–0.915	$P = 4$–6 kbar	22
Skaergaard: Upper Border Group	KG-57	0.940	0.587	0.933‡	0.9452–0.9462		$P = 600$ bars, Lindsley et al. (1969)	33
	KG-78	0.930	0.165	0.973		0.800–0.912		33
	KG-79	0.879	0.294	0.938	0.9436–0.9450			33
	KG-197	0.986	0.540	0.933‡	0.9482			33
	KG-247	0.893	0.659	0.941	0.9456–0.9474			33

C. Volcanic rocks with the assemblage fa + ilm + qtz

Locality	Sample no.	X_{Fa}	X_{ilm}	Remarks	Ref.†
Sierra la Primavera	174	0.935	0.947	most oxidizing rocks with fa + ilm + qtz	8
	37	0.932	0.959	most reducing rocks with fa + ilm + qtz	8
McDermitt caldera	CC-78-143	0.966	0.971	most oxidizing rocks with fa + ilm + qtz	31
	CC-78-140	0.97 (est.)	0.987	most reducing rocks with fa + ilm + qtz	31
Eastern Australia	9570	0.973	0.975	most oxidizing rocks with fa + ilm + qtz	10, 11
	155	0.976	0.982	most reducing rocks with fa + ilm + qtz	10, 11

D. Plutonic rocks with the assemblage fa + ilm + qtz

Locality	Sample no.	X_{Fa}	X_{ilm}	Remarks	Ref.†
Wolf River	TM-3	0.896	0.956	most oxidizing rocks with Fa + ilm + qtz	32
	GR-26A	0.933	0.976	most reducing rocks with Fa + ilm + qtz	32
Sybille	SR-136	0.928	0.952	most oxidizing rocks with Fa + ilm + qtz	20
	W-34-5-2	0.957	0.967	most reducing rocks with Fa + ilm + qtz	20

E. Plutonic rock with the assemblage fa + mag + qtz

Locality	Sample no.	X_{Fa}	X_{Usp}	Remarks	Ref.†
Skaergaard Sandwich Horizon	EG-4471	0.96–0.97 (est.)	0.855		19, 34

* Calculated by technique 1.
** Calculated by technique 2.
† References: 1–30, see Table 3; (31) Conrad, pers. comm.; (32) Anderson, 1975; (33) Naslund, 1980; (34) Brown and Vincent, 1963.
‡ Analysis of ilmenite has low total.

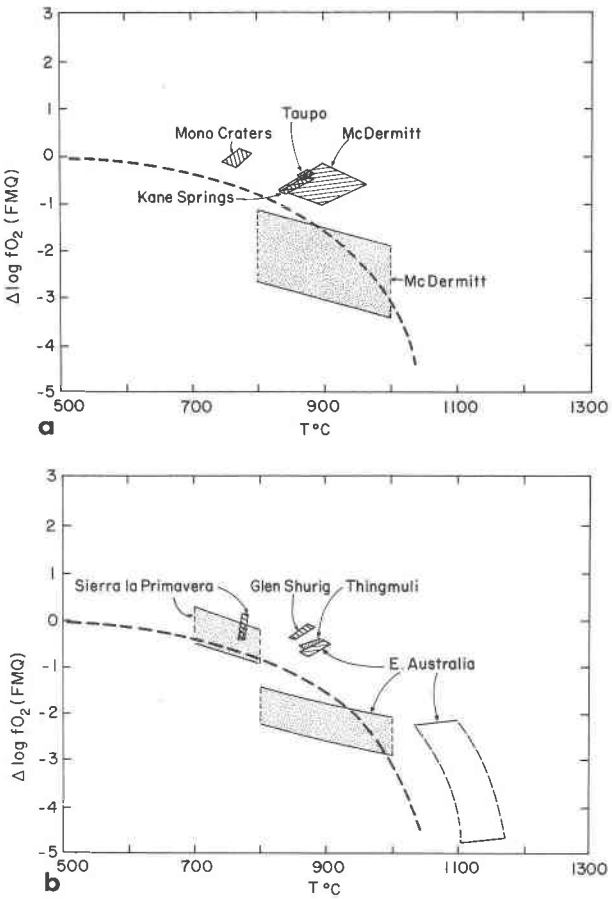

Fig. 7. Crystallization conditions for volcanic rocks containing fayalite and quartz. Solid lines outline inferred equilibrium conditions for rocks in which the olivine, ilmenite, and titanomagnetite have compositions that are consistent with the QUIIF equilibrium. Dashed lines show inferred conditions that were estimated from the compositions of olivine and ilmenite (technique 2). Stippled fields show ranges from assemblages olivine + ilmenite + quartz (technique 4); temperatures are assumed and in all cases are lower than the maximum values allowed by QUIIF.

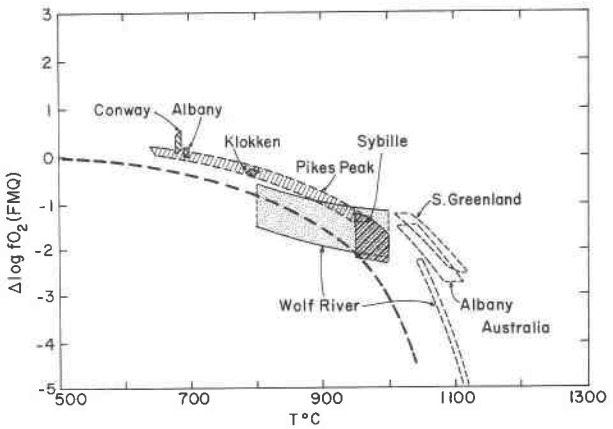

Fig. 8. Crystallization conditions inferred for fayalite-bearing plutonic rocks. Symbols as in Fig. 7.

did those that lack magnetite; the boundary between these assemblages is roughly consistent with the displaced position of the QUIIF surface. Several rock suites contain both magnetite-bearing and magnetite-absent assemblages, namely Sierra la Primavera, McDermitt caldera, the rhyolites of eastern Australia, the Sybille Monzosyenite, and the Wolf River batholith. Figures 7 and 8 show that the transition from titanomagnetite-bearing to titanomagnetite-absent assemblages in the very reduced rocks (the Australian rhyolites, Sybille Monzosyenite, and Wolf River batholith) could have occurred through cooling at a relatively fixed $\Delta \log f_{O_2}$. However, since the rocks from McDermitt caldera and Sierra la Primavera equilibrated at temperatures at which the QUIIF surface is relatively insensitive to changes in T, the major change in these rocks is likely to have been a relative decrease in f_{O_2}.

Figures 8 and 9 show that oxide-silicate re-equilibration persists in plutonic rocks to temperatures well below the solidus. Indeed, for most plutonic rocks, T and f_{O_2} cannot be recovered using technique 1. Even those rocks that do yield consistent results with technique 1 suggest temperatures well below those from other estimates. The Klokken Syenite, which yields the highest QUIIF temperatures of this set (800 °C), still seems to have re-equilibrated to temperatures at least 70 °C below the solidus (Parsons, 1981).

The manner in which plutonic rocks can re-equilibrate on cooling and the utility of the QUIIF equilibrium in describing these processes is particularly well displayed by the rocks from the Upper Border Group (UBG) and Sandwich Horizon of the Skaergaard intrusion (Fig. 9). The crystallization conditions of sample EG-4471 from the Sandwich Horizon were 600 bars and between 950 and 1030 °C (Lindsley et al., 1969). EG-4471 contains olivine (Fo_2) + magnetite ($Usp_{85.5}$) + quartz (Brown and Vincent, 1963; Vincent and Phillips, 1954). Complete olivine analyses are not given, but by comparison with the data of Naslund (1980), we estimate 1–2% tephroite and therefore a fayalite content of 96–97%. Using technique 4, we estimate that this sample would have equilibrated in the ruled area on Figure 9—in excellent agreement with the experimental work of Lindsley et al. (1969). Note that this—the one known exception to the rule that igneous rocks with fayalite + quartz also contain ilmenite (see previous discussion)—falls very close to QUIIF and thus was nearly ilmenite-saturated. Application of technique 2 to sample KG-78 of the UBG yields a maximum temperature and f_{O_2} very similar to those for EG-4471, a result implying that ilmenite is far more abundant than is magnetite in KG-78. Other samples from the UBG show a variety of QUIIF equilibration temperatures, indicating various degrees of subsolidus oxide-silicate re-equilibration—down to temperatures as low as 700 °C. [Ilmenites for two samples (KG-57, KG-197) show high calculated contents of Fe_2O_3; the analyses have low totals (Naslund, 1980) and are thus suspect. For these we as-

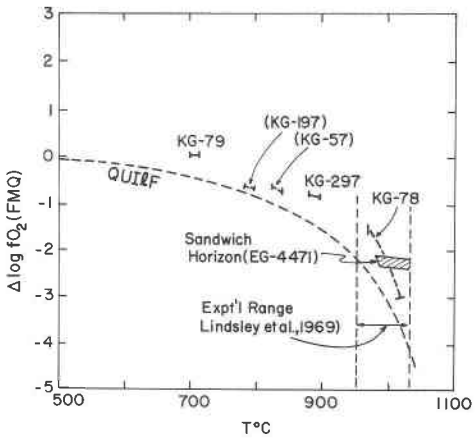

Fig. 9. Oxide-silicate re-equilibration trends as inferred for the Upper Border Group (based on the data of Naslund, 1984) and the Sandwich Horizon of the Skaergaard intrusion. Pressure is taken to be 600 bars (Lindsley et al., 1969). Solid lines give conditions estimated from ulvöspinel isopleths; dashed lines, those from ilmenite isopleths. Different samples re-equilibrated to different temperatures, but the close overall concordance with the QUIIF equilibrium strongly indicates a nearly closed system, with the oxides dominating the T-f_{O_2} trajectory upon cooling.

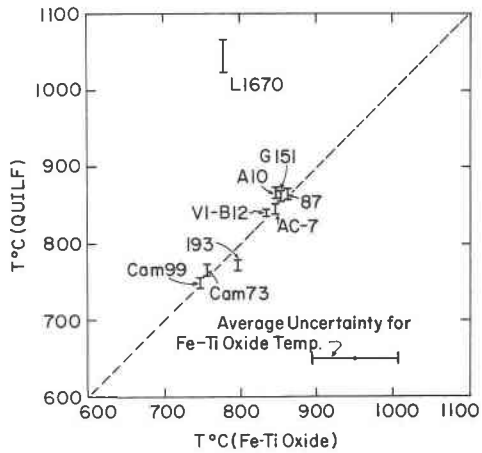

Fig. 10. A comparison of temperatures in volcanic rocks as estimated from two-oxide thermometry alone and from the QUIIF equilibrium.

sume that the magnetite compositions are primary; the corresponding maximum QUIIF equilibration temperatures are shown as dotted lines in Fig. 9.] Without further information it is difficult to say why the oxide-silicate equilibrium in the Skaergaard rocks shows such diverse lock-in temperatures, although possibly these represent varying degrees of interaction with external hydrothermal fluids (Taylor and Forester, 1979).

It is illuminating to compare the results of Fe-Ti oxide thermometry with those obtained using technique 1 and the QUIIF equilibrium (Fig. 10). The correlation for volcanic rocks is remarkable, even discounting the inherent error in the oxide temperatures. One can view the agreement as showing that the oxides alone provide adequate temperatures (albeit with larger uncertainties). A more pessimistic view would be that oxide-silicate re-equilibration is just as effective as oxide-oxide re-equilibration in these volcanic rocks—which we consider unlikely. The only volcanic sample that shows poor agreement is L1670, which contains an unusually titaniferous magnetite (X_{Usp} = 0.846). The QUIIF calculations indicate that the original spinel would have had to be even more Ti-rich (X_{Usp} = 0.9; Table 3). The QUIIF temperature for this sample strains credulity. We suggest that L1670 oxides re-equilibrated even during relatively rapid cooling as a consequence of this high Ti content. Indeed, it seems quite possible that this rock contained no primary ilmenite and that the reported ilmenite all formed by granule oxyexsolution; if so, the crystallization temperature and f_{O_2} for L1670 would have been very similar to those inferred for the Skaergaard Sandwich Horizon (Fig. 9) and the Sybille Monzosyenite (Fig. 8) and thus more plausible for this rock type.

Conclusions

The QUIIF equilibrium plays an important role in the relationships between oxide minerals and ferromagnesian silicates in Fe-rich igneous rocks. In rocks where the oxides control f_{O_2}, QUIIF will determine the T and f_{O_2} trajectory during differentiation or during oxide-silicate re-equilibration on cooling. If, however, the oxygen fugacity was controlled by some other assemblage or process, then magnetite will be eliminated by QUIIF during differentiation of a silica-saturated rock. Conversely, if differentiation is accompanied by decreasing silica activity, ilmenite will be eliminated from the rock by the QUIIF equilibrium.

The QUIIF equilibrium also has important uses in geothermometry. The assemblage magnetite + ilmenite + olivine + quartz is overdetermined in T-f_{O_2} space, which allows tighter constraints on those parameters than can be obtained from the two oxides alone, provided pressure is known or can be estimated to within a few kilobars. Furthermore, the QUIIF equilibrium is a sensitive indicator of resetting of one or both oxides and thus can be used to determine whether interoxide re-equilibration has occurred. QUIIF is, therefore, an important tool in helping the petrologist to see through the process of interoxide re-equilibration to estimate the conditions at which the oxides and silicates ceased to re-equilibrate.

Acknowledgments

We thank Jon Myers and Clara Podpora for assistance in the experimental portions of this study. We are especially indebted to C. Conrad, A. Ewart, M. Fuhrman, G. Mahood, and R. Naslund who provided unpublished analyses for inclusion in this paper; and to John Haas for providing his oxygen-buffer calibrations prior to publication. We thank Dennis Geist, James Munoz, and Douglas Rumble for perceptive and helpful reviews. This work was supported by NSF Grants EAR-8617812 (Frost) and by EAR-8416254 and EAR-8618480 (Lindsley).

References cited

Andersen, D.J., and Lindsley, D.H. (1981) A valid Margules formulation for an asymmetric ternary solution: Revision of the olivine-ilmenite

thermometer, with applications. Geochimica et Cosmochimica Acta, 45, 847–853.

——— (1988) Internally consistent solution models for Fe-Mg-Mn-Ti oxides: Fe-Ti oxides. American Mineralogist, 73, 714–726.

Anderson, J.L. (1975) Petrology and geochemistry of the Wolf River batholith. Ph.D. thesis, University of Wisconsin, Madison.

——— (1980) Mineral equilibria and crystallization conditions in the late Precambrian Wolf River rapakivi massif, Wisconsin. American Journal of Science, 280, 298–332.

Atkins, F.B. (1969) Pyroxenes of the Bushveld intrusion, South Africa. Journal of Petrology, 10, 222–249.

Barker, F., Wones, D.R., Sharp, W.N., and Desborough, G.A. (1975) The Pikes Peak batholith, Colorado Front Range, and a model for the origin of the gabbro–anorthosite–syenite–potassic granite suite. Precambrian Research, 2, 97–160.

Bizouard, H., Barberi, F., and Voret, J. (1980) Mineralogy and petrology of Erta Ale and Boina volcanic series, Afar Rift, Ethiopia. Journal of Petrology, 21, 401–436.

Bohlen, S.R., and Essene, E.J. (1977) Feldspar and oxide thermometry of granulites in the Adirondack Highlands. Contributions to Mineralogy and Petrology, 62, 153–169.

Bowen, N.L., and Schairer, J.F. (1935) The system MgO-FeO-SiO_2. American Journal of Science, 29, 151–217.

Brown, G.M., and Vincent, E.A. (1963) Pyroxenes from the late stages of fractionation of the Skaergaard Intrusion, East Greenland. Journal of Petrology, 4, 175–197.

Buddington, A.F., and Lindsley, D.H. (1964) Iron-titanium oxide minerals and synthetic equivalents. Journal of Petrology, 5, 310–357.

Carmichael, I.S.E. (1967a) The iron-titanium oxides of salic volcanic rocks and their associated ferromagnesian silicates. Contributions to Mineralogy and Petrology, 14, 36–64.

——— (1967b) The mineralogy of Thingmuli, a Tertiary volcano in eastern Iceland. American Mineralogist, 52, 1815–1841.

Conrad, W.K. (1984) The mineralogy and petrology of compositionally zoned ash flow tuffs and related silicic volcanic rocks, from the McDermitt caldera, Nevada-Oregon. Journal of Geophysical Research, 89, 8639–8664.

Davidson, P.M., and Mukhopadhyay, D.K. (1984) Ca-Fe-Mg olivines: Phase relations and a solution model. Contributions to Mineralogy and Petrology, 86, 256–263.

Duchesne, J.-C. (1972) Iron-titanium oxide minerals in the Bjerkem-Sogndal massif, South-western Norway, Journal of Petrology, 13, 57–81.

El Goresy, A., and Woermann, E. (1977) Opaque minerals as sensitive oxygen barometers and geothermometers in lunar basalts. In D.G. Fraser, Ed., Thermodynamics in geology, p. 249–277. D. Reidel, Boston, Massachusetts.

Ewart, A. (1981) The mineralogy and chemistry of the anorogenic Tertiary silicic volcanics of S. E. Queensland and N. E. New South Wales, Australia. Journal of Geophysical Research, 86, 10242–10256.

Ewart, A., Hildreth, W., and Carmichael, I.S.E. (1975) Quaternary acid magmas in New Zealand. Contributions to Mineralogy and Petrology, 51, 1–27.

Ferguson, A.K. (1978) A mineralogical investigation of some trachyte lavas and associated pegmatoids from Camel's Hump and Turritable Falls, central Victoria. Journal of the Geological Society of Australia, 25, 185–197.

Floran, R.J., and Papike, J.J. (1978) Mineralogy and petrology of the Gunflint Iron Formation, Minnesota-Ontario: Correlation of compositional and assemblage variation at low to moderate grades. Journal of Petrology, 19, 215–288.

Frisch, T., and Bridgwater, D. (1976) Iron- and manganese-rich minor intrusions emplaced under late-orogenic conditions in the Proterozoic of South Greenland. Contributions to Mineralogy and Petrology, 57, 25–48.

Frost, B.R. (1982) Contact effects of the Stillwater Complex, Montana: The concordant iron-formation: A discussion of the role of buffering in metamorphism of iron formation. American Mineralogist, 67, 142–148.

——— (1985) On the stability of sulfides, oxides, and nature metals in serpentinite. Journal of Petrology, 26, 31–63.

Fuhrman, M.L., Frost, B.R., and Lindsley, D.H. (1988) The crystallization conditions of the Sybille Monzosyenite, Laramie Anorthosite Complex, Wyoming. Journal of Petrology, in press.

Haggerty, S.E. (1976) Opaque mineral oxides in terrestrial igneous rocks. Mineralogical Society of America Reviews in Mineralogy, 3, Hg-101–Hg-300.

Larsen, N.M. (1976) Clinopyroxenes and coexisting mafic minerals from the alkaline Ilimaussaq intrusion, South Greenland. Journal of Petrology, 17, 258–290.

Lindsley, D.H., Brown, G.M., and Muir, I.D. (1969) Conditions of the ferrowollastonite-ferrohedenbergite inversion in the Skaergaard intrusion, East Greenland. Mineralogical Society of America Special Paper 2, 193–201.

Mahood, G.A. (1981) Chemical evolution of a Pleistocene rhyolite center: Sierra La Primavera, Jalisco, Mexico. Contributions to Mineralogy and Petrology, 77, 129–149.

Mitchell, R.H., and Platt, R.G. (1978) Mafic mineralogy of ferroaugite syenite from Coldwell alkaline complex, Ontario, Canada. Journal of Petrology, 19, 627–651.

Morse, S.A. (1980) Kiglapait mineralogy: II. Fe-Ti oxide minerals and the activities of oxygen and silica. Journal of Petrology, 21, 685–719.

Naslund, H.R. (1980) Part I. Petrology of the Upper Border Group of the Skaergaard intrusion, East Greenland. Part II. An experimental study of liquid immiscibility in iron-bearing silicate melts. Ph.D. dissertation, University of Oregon, Eugene.

——— (1984) Petrology of the upper border series of the Skaergaard intrusion. Journal of Petrology, 23, 185–212.

Nicholls, J., Carmichael, I.S.E., and Stormer, J.C. (1971) Silica activity and P_{total} in igneous rocks. Contributions to Mineralogy and Petrology, 33, 1–20.

Novak, S.W., and Mahood, G.A. (1986) Rise and fall of a basalt-trachyte-rhyolite magma system at Kane Springs Wash caldera, Nevada. Contributions to Mineralogy and Petrology, 94, 352–373.

Ohmoto, H., and Kerrick, D.M. (1977) Devolatilization equilibria in graphitic schists. American Journal of Science, 277, 1013–1044.

Osborn, E.F. (1959) Role of oxygen pressure in the crystallization and differentiation of basaltic magma. American Journal of Science, 257, 609–647.

Parsons, I. (1981) The Klokken Gabbro-Syenite Complex, South Greenland: Quantitative interpretation of mineral chemistry. Journal of Petrology, 22, 233–260.

Powell, M. (1978) The crystallization history of the Igdlerfigssalik nepheline syenite intrusion, Greenland. Lithos, 11, 99–120.

Rumble, D., III (1970) Thermodynamic analysis of phase equilibria in the system Fe_2TiO_4-Fe_3O_4-TiO_2. Carnegie Institution of Washington Year Book 69, 198–207.

Simons, B., and Woermann, E. (1978) Iron-titanium oxides in equilibrium with metallic iron. Contributions to Mineralogy and Petrology, 66, 81–89.

Stephenson, N.C.N., and Hensel, H.D. (1978) A Precambrian fayalite granite from the south coast of Western Australia. Lithos, 11, 209–218.

Taylor, H.P., and Forester, R.W. (1979) An oxygen and hydrogen isotope study of the Skaergaard intrusion and its country rocks: A description of a 55-m.y.-old fossil hydrothermal system. Journal of Petrology, 20, 355–419.

Taylor, L.A., Williams, R.J., and McCallister, R.H. (1972) Stability relations of ilmenite and ulvöspinel in the Fe-Ti-O system and application of these data to lunar mineral assemblages. Earth and Planetary Science Letters, 16, 282–288.

Thy, P. (1982) Titanomagnetite and ilmenite in the Fongen-Hyllingen Complex, Norway. Lithos, 15, 1–16.

Upton, B.J.G., and Thomas, J.E. (1980) The Tugtutoq younger dyke complex, South Greenland: Fractional crystallization of transitional olivine basalt magma. Journal of Petrology, 21, 167–198.

Upton, B.J.G., Stephenson, D., and Martin, A.R. (1985) The Tututoq older Dyke Complex: Mineralogy and geochemistry of an alkali gabbro–augite syenite–foyaite association in the Gadar Province of South Greenland. Mineralogical Magazine, 49, 623–642.

Vincent, E.A., and Phillips, R. (1954) Iron-titanium oxide minerals in layered gabbros of the Skaergaard intrusion, East Greenland. Geochimica et Cosmochimica Acta, 6, 1–26.

Whitney, J.A., and Stormer, J.C., Jr. (1976) Geothermometry and geobarometry in epizonal granitic intrusions: A comparison of iron-titanium oxides and coexisting feldspars. American Mineralogist, 61, 751–761.

Wolff, J.A., and Wright, J.V. (1981) Formation of the Green Tuff, Pantelleria, Bulletin Volcanologique 44, 681–690.

Manuscript received August 31, 1987
Manuscript accepted March 21, 1988

Appendix 1. Experimental details

Starting materials for the experiments locating the QUIIF equilibrium were synthetic phases made from high-purity reagents: SiO_2, Alfa #060580, 99.999%; Fe^0 sponge, J.M. # S81214C, 99.999%; Fe_2O_3, J.M. # S.85283A, 99.999%; TiO_2, J.M. # 810420, 99.995%; and Fe wire (for capsules), J.M. # W 9530, 99.998%. Reagents were carefully dried before weighing; the Fe^0 sponge was analyzed for oxygen content and the proportions of sponge and Fe_2O_3 adjusted accordingly. Mixes were ground in an agate mortar; Fe^0 sponge was added near the end of the grinding process to minimize oxidation. Fe-Ti spinels and ilmenite solid solutions were synthesized dry at 930 °C in evacuated silica-glass tubes lined with Ag foil. Fayalite was made from Fe_2O_3 and SiO_2 at 1100 °C in a CO-CO_2 atmosphere adjusted to be about one log unit above the IFQ reaction.

Point Q (the assemblage SiO_2 + Usp + Ilm + Fay + Fe^0) was determined by reacting equimolar mixtures of Fay + Ilm and of Usp + Qtz in Fe^0 capsules that were sealed in evacuated silica-glass tubes; the assemblages were self-buffering. At 1050 °C, Fay + Ilm grew from Usp + Qtz; at 1060 °C, Usp + Qtz grew from Fay + Ilm (+ qtz seeds).